scientific reports

OPEN

Comprehensive profiling of plasma and exosomal microRNAs in medication-related osteonecrosis of the jaw

Sujin Oh[1], Minjae Park[2], Hyun Hwang[3], Jung-Hyun Park[4], Keun-Suh Kim[5], Jin-Woo Kim[3,4,6]✉ & Hyo-Jung Lee[5]✉

The role of circulating microRNAs (miRNAs) in the pathophysiology of medication-related osteonecrosis of the jaw (MRONJ) remains to be elucidated. This study investigated the expression of plasma miRNAs in patients with MRONJ compared to healthy individuals. 16 patients with MRONJ and 15 healthy controls participated in this case-control study, which was conducted in three consecutive phases. As a pilot study, miRNA profiling was performed using quantitative real-time reverse transcriptase PCR (qPCR) array plates targeting 754 miRNAs in a subset of plasma samples. In the subsequent phases, individual qPCR assays validated the array results using plasma samples from the full cohort (second phase) and plasma-derived exosomes (third phase). The qPCR arrays revealed differential miRNA profiles between the MRONJ and control groups. We selected miR-153-3p, miR-1180-3p, miR-483-5p, miR-511-5p, miR-628-3p, miR-486-5p, miR-92b-5p, miR-16-3p, miR-23a-3p, and miR-23a-5p for additional assays. The expression of miR-483-5p, miR-92-5p, and miR-486-5p was elevated in patients with MRONJ compared to controls, whereas miR-628-3p was downregulated ($q < 0.01$). All four miRNAs consistently exhibited differences in expression in plasma-derived exosomes between MRONJ patients and controls. We identified four miRNAs that could serve as potential biomarkers for MRONJ: miR-483-5p, miR-92-5p, miR-628-3p, and miR-486-5p. These biomarkers may reflect key pathways in MRONJ pathogenesis and could be used to guide patient risk stratification and future therapeutic interventions for MRONJ.

Keywords Medication-related osteonecrosis of the jaw, Circulating microRNA, Plasma-derived exosomes, Quantitative real-time PCR, Gene expression profiling

Medication-related osteonecrosis of the jaw (MRONJ) is an adverse drug reaction associated with antiresorptive or antiangiogenic treatments. It is characterized by the exposure of the jawbones, including the mandible and maxilla, through an extra or intraoral fistula that persists for > 8 weeks[1]. Antiresorptive agents, such as bisphosphonates and denosumab, are prescribed for patients with osteoporosis or bone-destructive cancers, such as multiple myeloma and bone metastases of solid tumors. Incidences of MRONJ differ markedly by indication and dosing regimen. Among patients treated for osteoporosis, the risk is relatively low –approximately 0.01–0.05% with oral bisphosphonates and 0.04–0.3% with denosumab[2,3]. By contrast, in cancer patients receiving high-dose intravenous antiresorptive, cumulative MRONJ incidence is substantially higher, typically 0.7–5.4%[2,3], and up to 13% in some metastatic breast cancer cohorts or patients undergoing sequential antiresorptive therapy[4,5].

Multiple hypotheses have been proposed to explain MRONJ since it was first described in 2003[6]. Current evidence supports a 'multiple-strike' model in which immune dysregulation increases susceptibility to oral

[1]Department of Laboratory Medicine, Seoul National University College of Medicine, Seoul, Republic of Korea. [2]Seoul National University College of Medicine, Seoul, Republic of Korea. [3]Graduate School of Medicine, Ewha Womans University, Seoul, Republic of Korea. [4]Department of Oral and Maxillofacial Surgery, School of Medicine, Ewha Womans University, Seoul, Republic of Korea. [5]Department of Periodontology, Section of Dentistry, Seoul National University Bundang Hospital, 82, Gumi-ro 173beon-gil, Bundang-gu, Gyeonggi-do, Seongnam 13620, Republic of Korea. [6]Department of Oral & Maxillofacial Surgery, School of Medicine, Ewha Womans University, Ewha Womans University Seoul Hospital, 25, Magokdong-ro 2-gil, Gangseo-gu, Seoul 07804, Republic of Korea. ✉email: jinu600@gmail.com; periolee@gmail.com

dysbiosis and infection, amplifying chronic inflammation; in parallel, suppressed bone remodeling and angiogenesis impair healing and clearance of necrotic bone after dentoalveolar injury. These interacting processes, modulated by drug type, cumulative dose and route, as well as host factors, are thought to converge to produce MRONJ[3,7,8]. Nevertheless, the precise pathophysiological pathways remain unproven, underscoring the need for further research. Although many molecules (e.g. markers of bone turnover) have been investigated as potential biomarkers, no reliable biomarker for MRONJ has yet been identified[9].

MicroRNAs (miRNAs) are short, non-coding RNAs that post-transcriptionally regulate gene expression[10,11]. Beyond their broad roles in cell differentiation and immunity, specific miRNAs modulate osteoclast and osteoblast activity[12], inflammatory pathways[13], and angiogenesis[14]. After intracellular maturation, miRNAs are released extracellularly either within exosomes or bound to RNA-binding proteins, which confers stability in biofluids and enables detection in plasma and saliva[15,16]. Exosomes derived from osteoclasts/osteoblasts, endothelial, and immune cells in the oromaxillary bone microenvironment can carry miRNAs that reflect local injury, infection-driven inflammation, and impaired bone remodeling or angiogenesis implicated in MRONJ. These features collectively support circulating or exosomal miRNAs as plausible, minimally invasive biomarkers for MRONJ risk stratification, disease detection, and monitoring of healing status, motivating their evaluation in the present study.

Regarding MRONJ, only a few studies have identified changes in miRNA expression and their role in pathogenesis[17]. Some previous studies have used circulating miRNA panels as a biomarker for MRONJ diagnosis, generating a logistic regression model that predicts MRONJ according to the relative expressions of multiple miRNAs[18,19]. Certain miRNAs, such as miR-23a and miR-21, target genes involved in the differentiation and regulation of bone cells, thereby affecting bone remodeling[20,21]. However, few studies have investigated this topic, and expression profiles tend to differ depending on the detection and analysis methods employed.

We investigated the expression of plasma miRNAs in MRONJ patients and healthy individuals. Using a carefully designed PCR-based miRNA quantification approach and advanced algorithms, we selected and validated miRNAs with differential expression in MRONJ patients compared to controls. We also examined the consistency of miRNA expression in both plasma samples and plasma-derived exosomes. We identified specific miRNAs associated with MRONJ and propose these as novel biomarkers for the disease, with the potential to improve risk assessment and deepen our understanding of MRONJ pathogenesis.

Materials & methods

Participants

This study included 16 patients diagnosed with MRONJ, who visited the dental clinic of Seoul National University Bundang Hospital (SNUBH) or Ewha Womans University Mokdong Hospital between December 2021 and August 2022. The diagnosis of MRONJ was made after conducting a thorough medical history, dental examination, and imaging studies based on the guideline published by the American Association of Oral and Maxillofacial Surgeons[1]. The cohort size reflects all consecutive eligible and consenting cases within the defined recruitment period. Demographic and clinical features of the patients were documented including initial staging, cause of MRONJ, and details about medication regimens. For antiresorptive therapy, data were abstracted from the medical record, including the indication, agent, route of administration, nominal dose, dosing interval (application interval), and treatment start/stop dates, from which total treatment duration was calculated; per-patient details are provided in Supplementary Table S1. For the control group, 15 healthy individuals were recruited from visitors to the SNUBH dental clinic. Eligibility criteria required no history of malignancy, no prior or current exposure to oral or intravenous bisphosphonates, denosumab, or anti-angiogenic therapies, and no prior MRONJ. To minimize peri-enrollment bias, individuals with recent oral surgery or tooth extraction (within the preceding 6 months) or clinical evidence of active oral infection were excluded. A structured questionnaire captured age, sex, diabetes mellitus, cardiovascular disease, chronic systemic steroid exposure, smoking, and alcohol use. Controls were not matched to cases; instead, we compared baseline characteristics between groups. The clinical data of study participants are listed in Tables 1 and 2.

All study procedures were approved by the Institutional Review Boards (IRBs) of SNUBH and Ewha Womans University Medical Center and conducted in accordance with the Declaration of Helsinki (IRB number: B-2001-589-301 and 2021-11-020-004). All subjects provided written informed consent.

Study design

A case-control design was applied. In accordance with best practices for observational studies, we have followed the Strengthening the Reporting of Observational Studies in Epidemiology (STROBE) guidelines[22]. A completed STROBE checklist has been included in Supplementary Tables 1 to ensure transparency and comprehensiveness in reporting.

This study was conducted in three consecutive phases (Fig. 1). In the first phase, as a pilot feasibility step, we profiled 754 miRNAs on quantitative real-time reverse transcriptase PCR (qPCR) array plates using five randomly selected plasma samples from each group. miRNAs showing higher expression in MRONJ samples compared to controls were flagged as preliminary differentially expressed (DE) candidates. In addition, those that showed stable expression across subjects, assessed by the geNorm stability score[23], were selected as candidate reference genes (RGs) to serve as endogenous controls for normalizing the expression levels of genes of interest (GOIs).

To reduce false discovery and enhance biological relevance, we integrated the Phase-1 list with a literature-based list of miRNAs previously associated to osteoclast/osteoblast pathways or inflammatory regulation. We also added miRNAs with specific evidence of elevated expression in ONJ patients —even if not detected in the initial phase—as GOIs for subsequent experiments. RGs were also selected based on their use as controls in prior miRNA quantification studies.

Characteristics		Control (*N* = 15)	MRONJ (*N* = 16)	*P*-value
Age (y)	Mean ± SD	62.2 ± 7.4	74.2 ± 9.0	< 0.001
Sex	N (%)			1.000
	M	0 (0.0)	0 (0.0)	
	F	15 (100.0)	16 (100.0)	
Diabetes mellitus	N (%)			0.172
	Yes	1 (6.7)	5 (31.2)	
	No	14 (93.3)	11 (68.8)	
Chronic steroid exposure	N (%)			1.000
	Yes	0 (0.0)	0 (0.0)	
	No	15 (100.0)	16 (100.0)	
Alcohol consumption	N (%)			< 0.001
	Yes	10 (66.7)	0 (0.0)	
	No	5 (33.3)	16 (100.0)	
Smoking	N (%)			1.000
	Yes	0 (0.0)	0 (0.0)	
	No	15 (100.0)	16 (100.0)	
Cardiovascular diseases	N (%)			1.000
	Yes	1 (6.7)	1 (6.2)	
	No	14 (93.3)	15 (93.8)	

Table 1. Baseline demographics and clinical characteristics of healthy controls and patients with medication-related osteonecrosis of the jaw (MRONJ). M, male; F, female.

In the second phase, the expression of the candidate miRNAs was validated by conducting qPCR assays of plasma samples across all subjects. 14 miRNA targets were assessed, including 10 GOIs and 4 candidate RGs, resulting in the identification of five significant DE miRNAs and two stable RGs.

Finally, we examined the expression of the identified miRNAs in plasma-derived exosomal fractions to verify whether the changes in gene expression observed in plasma were consistently reflected in exosomes. This approach aimed to enhance the robustness of these miRNAs for use as potential biomarkers.

Sample collection

Blood samples were collected from each participant by trained personnel using 4 mL EDTA whole blood tubes. The samples were centrifuged to obtain plasma aliquots. All samples were promptly transported to the laboratory and stored at − 80 °C until further analysis.

Exosome isolation and MiRNA extraction

The PHiCS Institute (Seoul, Korea) performed sample preparation and PCR experiments. Two types of miRNA sample (plasma miRNA and plasma-derived exosomal miRNA) were used. Exosomes were isolated from plasma samples using the miRCURY Exosome Serum/Plasma Kit (Qiagen, Hilden, Germany) in accordance with the manufacturer's instructions. miRNA was extracted from all samples and their exosome isolates using the miRNeasy Serum/Plasma Advanced Kit (Qiagen), following the manufacturer's guidelines. RNA concentration was measured using a Nanodrop spectrophotometer (Nabi MicroDigital Co., Ltd., Korea).

qPCR array plate-based MiRNA profiling

Reverse transcription (RT) was performed with universal RT primers following poly(A) tailing and adapter ligation of miRNAs using the TaqMan Advanced miRNA cDNA Synthesis Kit (Applied Biosystems, Foster City, CA, USA) according to the manufacturer's protocols. Complementary DNA (cDNA) templates were subjected to real-time PCR using TaqMan Advanced miRNA Human A and B Plates (Applied Biosystems), which are designed to amplify 754 human miRNAs, with TaqMan Fast Advanced Master Mix (Applied Biosystems). PCR reactions were performed on a QuantStudio 3 system (Applied Biosystems) with the following conditions: an initial denaturation step at 95 °C for 20 s, followed by 40 cycles of 95 °C for 1 s and 60 °C for 20 s.

Individual qPCR assays for validation of expression profiles

qPCR assays of the selected miRNA targets were performed using TaqMan MicroRNA Assays (Applied Biosystems) according to the manufacturer's protocols. RNA samples were reverse transcribed with pools of stem-loop structured miRNA-specific RT primers using the TaqMan MicroRNA Reverse Transcription Kit (Applied Biosystems), followed by a preamplification step. cDNA standard was prepared using RNA pooled from randomly selected samples. Real-time PCR was conducted using each TaqMan Assay with the TaqMan Fast Advanced Master Mix (Applied Biosystems). Reactions were performed on a QuantStudio 3 system (Applied Biosystems) with the following conditions: an initial denaturation step at 95 °C for 20 s, followed by 40 cycles of 95 °C for 1 s and 60 °C for 20 s. Five five-fold serial dilutions of cDNA standard were prepared and used in parallel with test samples for each assay to establish a standard curve for calculating PCR efficiency. Test

Features		MRONJ (*N* = 16)
Initial stage of MRONJ	N (%)	
I		5 (31.2)
II		11 (68.8)
Anatomical location	N (%)	
Maxilla		5 (31.2)
Mandible		11 (68.8)
Indication for antiresorptive therapy	N (%)	
Osteoporosis		15 (93.8)
Cancer		1 (6.2)
Type of antiresorptive	N (%)	
Alendronate		1 (6.7)
Ibandronate		3 (20.0)
Risedronate		2 (13.3)
Zoledronate		2 (13.3)
Denosumab		3 (20.0)
Ibandronate + Risedronate		1 (6.7)
Ibandronate + Denosumab		1 (6.7)
Ibandronate + Zoledronate		1 (6.7)
Risedronate + Denosumab		1 (6.7)
Route of administration	N (%)	
PO		5 (31.2)
IV		6 (37.5)
IV + PO		5 (31.2)
Duration of administration (months)	Mean ± SD	43.5 ± 29.4
Cause of MRONJ	N (%)	
None		1 (6.2)
Dental Extraction		6 (37.5)
Periodontitis		1 (6.2)
Dental Implant		4 (25.0)
Dental Extraction + Periodontitis + Dental Implant		1 (6.2)
Dental Extraction + Denture + Periodontitis		1 (6.2)
Dental Extraction + Dental Implant		2 (12.5)

Table 2. Clinicopathological features of patients with medication-related osteonecrosis of the jaw (MRONJ). PO, per oral; IV, intravenous.

samples were run on one plate for a single assay, and each run included cDNA standards (5-fold dilutions), inter-run calibrators (IRCs), no template control (NTC), and the samples. IRCs consisted of two wells containing undiluted cDNA standard for miR-221-3p and miR-21-5p assays in each run. These identical samples served as calibrators across all runs, allowing for the calculation of correction factors to adjust for inter-run variation.

Bioinformatics analysis

Relative quantification of miRNA expression was conducted with the qBase + software (Biogazelle, Zwijnaarde, Belgium) using PCR cycle threshold (Ct) values[24]. "Undetermined" data points were assigned a Ct value of 40 to enable calculation of quantities. The PCR efficiency (E) for each target was determined by plotting the Ct values on the y-axis against the logarithm of the input concentration of 5-fold-diluted cDNA standards on the x-axis and calculated as $E = 5^{-1/\text{slope}}$. The stability of miRNA expression was evaluated using the geNorm algorithm, which calculates each gene's stability measure (M) by averaging its pairwise variation in relative quantities (RQs) with all other genes. Genes with M values < 0.5 were considered to have high levels of stability. RGs were selected according to their gene stability values and were used to normalize GOI expression. The qBase + algorithm, which allows implementation of up to five multiple RGs, was applied to calculate the normalized RQ (NRQ) of each target miRNA in each sample[24]; the RQ for each gene was derived from the Ct values using the formula $RQ = E^{\Delta Ct}$, where ΔCt is the difference in Ct between each sample and the baseline, i.e., the average values of all samples. The NRQ for each sample was calculated by dividing each RQ by the normalization factor (NF), i.e., the geometric mean of the RQs of the selected RGs. When no gene met the stability criterion for RG selection, the geometric mean of the RQs from all target miRNAs was used as the NF for each sample. For validation assays

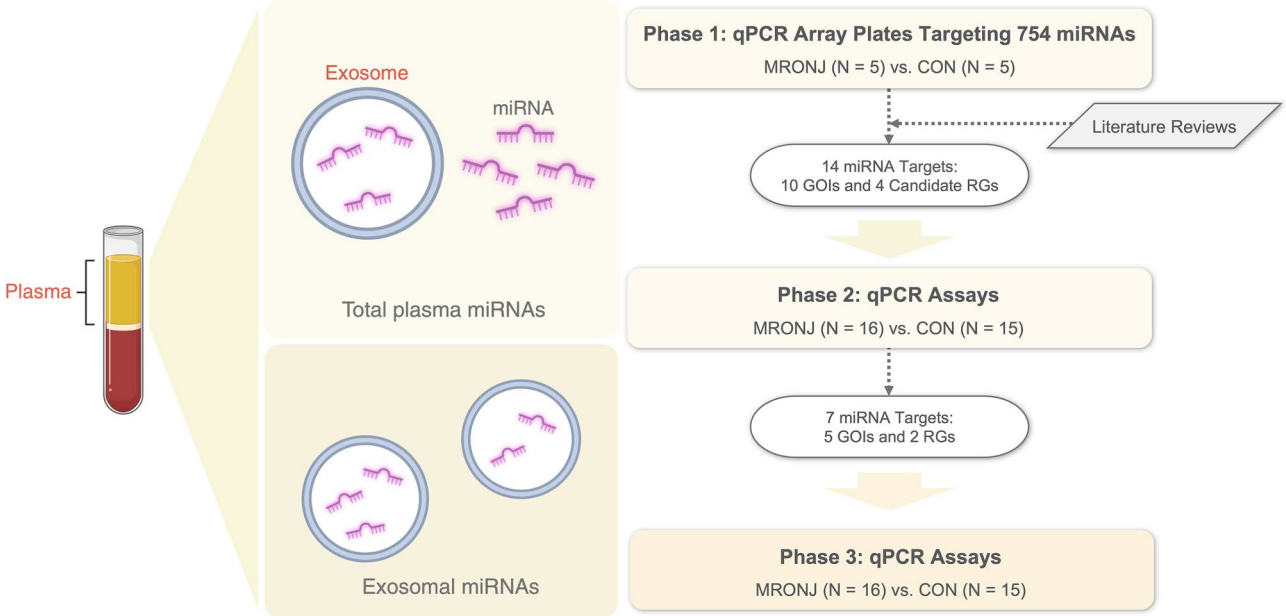

Fig. 1. Schematic of the study design. This study was divided into three consecutive phases. For the first phase, a pilot study, microRNA (miRNA) profiling was conducted with a small number of plasma samples using quantitative real-time reverse transcriptase PCR (qPCR) array plates targeting 754 miRNAs. Results from the first-phase experiment and a literature review were combined to select candidate genes for the subsequent phase. In the second phase, the expression of the selected miRNA targets was validated through individual qPCR assays using total plasma samples from a full cohort. For the third phase, plasma-derived exosome samples underwent individual qPCR assays to verify whether changes in miRNA expression were consistently observed in exosomes (MRONJ, medication-related osteonecrosis of the jaw; CON, control; GOI, gene of interest; RG, reference gene). Created in https://BioRender.com.

where IRCs were included in each run, the calibrated NRQ (CNRQ) of each sample was calculated by dividing each NRQ by the calibration factor (CF), i.e., the geometric mean of the NRQs of the IRCs.

Statistical analysis

All statistical analyses and data visualizations were conducted using R software (version 4.2.2; R Development Core Team, Vienna, Austria). Associations between categorical variables were assessed using either the chi-square test or Fisher's exact test, depending on the data distribution. Differences in continuous variables between the MRONJ and control groups were evaluated using Student's t-test for parametric distributions and the Wilcoxon rank-sum test for nonparametric distributions. Multiple testing corrections were applied using the Benjamini–Hochberg (BH) method. Statistical significance was defined as a p-value < 0.05 or a q-value < 0.05. Log fold change (logFC) was calculated by subtracting the mean log-scaled NRQ or CNRQ value of the control group from the mean value of the MRONJ group. Unsupervised hierarchical clustering was conducted on the Euclidean distances of CNRQ values using average linkage to evaluate the presence of distinct clusters and their correspondence with the previously defined control and MRONJ groups. To evaluate the consistency of miRNA dysregulation across sample types (total plasma and plasma-derived exosomes), linear mixed-effects models were applied for each DE miRNA using the *lme4* R package[25]. The model included CNRQ values as the dependent variable and subject-specific random effects with fixed effects for the subject group (controls vs. MRONJ) and sample type (plasma vs. exosome), and the interaction between the subject group and sample type. The statistical result for the interaction term was used to determine whether the effect of the subject group on the expression of each gene differed between plasma and exosome samples.

Results

Patient characteristics

This study included 16 patients with MRONJ and 15 healthy controls, and their clinical information is summarized in Tables 1 and 2. The mean ± SD age was 74.2 ± 9.0 years in MRONJ patients and 62.2 ± 7.4 years in controls ($p < 0.001$). All participants were female. At initial staging, five MRONJ patients were classified as Stage I and eleven were Stage II; no Stage III cases were enrolled during the study period. Osteonecrosis occurred in the maxilla in five patients and in the mandible in 11 patients. Antiresorptive treatment was prescribed primarily for osteoporosis in 15 patients and for cancer in one patient. The types of antiresorptive agents used included denosumab ($n = 3$), single bisphosphonates ($n = 8$), two different types of bisphosphonate ($n = 2$), or a combination of denosumab and bisphosphonates ($n = 2$). Drug administration routes were oral ($n = 5$), intravenous ($n = 6$), or both ($n = 5$) with an average treatment duration of 43.5 ± 29.4 months.

Phase 1: expression profiles of plasma MiRNAs

The expression profiles of 754 miRNAs were investigated. According to the geNorm analysis, 11 miRNAs exhibited a high level of gene stability (M < 0.5), and the five most stably expressed genes (miR-138-30p, miR-148b-3p, miR-152-3p, miR-186-5p, and miR-221-3p) were selected as RGs for normalization of RQs (Fig. 2A). Statistical analysis of NRQ values revealed 26 DE miRNAs between the patient and control groups (Fig. 2B and Supplementary Table 2). Among them, 11 genes (miR-153-3p, miR-1180-3p, miR-483-5p, miR-511-5p, miR-628-3p, miR-486-5p, miR-92b-5p, miR-500a-3p, miR-9-3p, let-7b-3p, and let-7e-5p) were highly upregulated in MRONJ patients compared to controls (Wilcoxon, $p < 0.05$; FC > 2). Because miRNA is sparsely detected in plasma, genes that showed increased expression in the patient group were considered GOI targets for the next phase of the study. Detailed results are shown in Table 3.

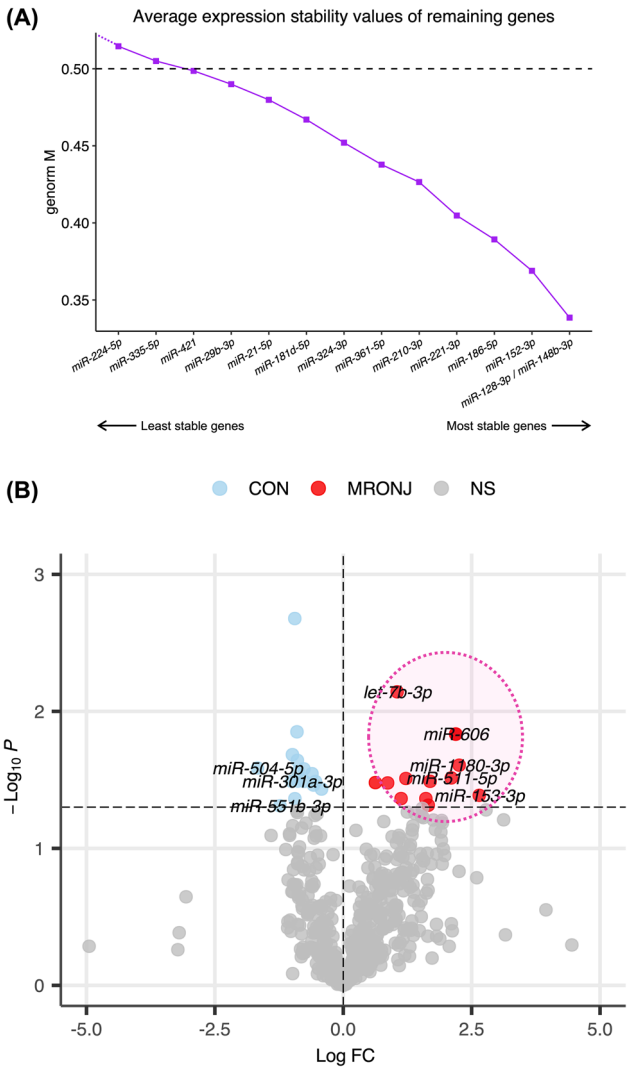

Fig. 2. Plasma microRNA (miRNA) profiles of patients with medication-related osteonecrosis of the jaw (MRONJ) and healthy controls obtained from quantitative real-time reverse transcriptase PCR (qPCR) array plates. (**A**) Gene expression stability of target miRNAs according to the geNorm algorithm. Expression stability was evaluated using gene stability measure (M) values. The figure specifically focuses on a subset of miRNAs identified from the full set of qPCR array targets, providing a detailed view of the most stable miRNAs. The dotted line shows the cut-off for genes with highly stable expression (M < 0.5). Eleven miRNA targets were highly stable, and the five most stably expressed genes were selected as reference genes. (**B**) Volcano plot demonstrating differential expression of plasma miRNAs between the MRONJ and control (CON) groups. Blue dots represent miRNAs downregulated in the MRONJ group compared to the control group, while red dots indicate upregulated miRNAs ($p < 0.05$). Among these, 11 genes (shaded red circles) that showed significant upregulation (fold change [FC] > 2 and $p < 0.05$) in the MRONJ group were selected as potential targets for validation assays in the second phase (NS, not significant).

Gene	*P*-value*	Q-value*	FC† (MRONJ/CON)	95% CI low	95% CI high
miR-153-3p	0.041	0.697	14.119	1.180	168.888
miR-1180-3p	0.025	0.697	9.559	1.476	61.916
miR-483-5p	0.015	0.697	8.935	1.794	44.494
miR-511-5p	0.031	0.697	8.194	1.374	48.876
miR-628-3p	0.032	0.697	5.424	1.247	23.588
miR-486-5p	0.048	0.697	5.236	1.017	26.965
miR-92b-5p	0.043	0.697	4.993	1.077	23.163
miR-500a-3p	0.031	0.697	3.385	1.159	9.892
miR-9-3p	0.043	0.697	3.084	1.047	9.087
let-7b-3p	0.007	0.697	2.856	1.513	5.390
let-7e-5p	0.033	0.697	2.374	1.092	5.158

Table 3. Expression profiles of plasma MicroRNAs (miRNAs) significantly upregulated in patients with medication-related osteonecrosis of the jaw (MRONJ) compared to controls using qPCR array plates. FC, fold change; CON, control; CI, confidence interval. *Differentially abundant miRNAs were determined using the Wilcoxon rank-sum test, with correction for multiple testing performed using the Benjamini–Hochberg (BH) method. Statistical significance was determined as a p-value < 0.05. †The FC value of each gene represents how many times the mean expression level in the MRONJ group is compared to the mean expression level in the control group. The 95% CIs of FC values were calculated. Only genes with a fold change (FC) of ≥ 2 were selected as targets for the subsequent experiments.

Review of previous MiRNA studies

We reviewed the literature to identify miRNAs previously reported to be associated with MRONJ. Among the 11 upregulated genes from the array results, five miRNAs (miR-153-3p, miR-483-5p, miR-628-3p, miR-486-5p, and miR-92b-5p) showed evidence of an association with inflammation or bone remodeling. Specifically, miR-153-3p, miR-483-5p, miR-628-3p, and miR-92b-5p were implicated in bone turnover via the modulation of osteogenic and/or osteoclastic differentiation[26–31]. miR-486-5p was found to play a significant role in regulating inflammation by modulating oxidative stress and cytokine production[32,33]. Furthermore, three additional miRNAs that showed increased expression in MRONJ patients in previous studies (miR-16-3p, miR-23a-3p, and miR-23a-5p) were selected as GOIs for a subsequent validation assay[18,19,28]. Among the five RGs chosen in the pilot study, miR-21-5p and miR-221-3p, which have been used as endogenous controls in previous studies, were selected for inclusion in this assay[34,35]. Two other miRNAs, miR-16-5p and miR-26a-5p, which are widely adopted as RGs for PCR-based miRNA quantification, were also added as candidate RGs[34–39],

Phase 2: validation of DE MiRNAs

qPCR assays targeting 14 miRNAs, consisting of 10 GOIs (miR-153-3p, miR-1180-3p, miR-483-5p, miR-511-5p, miR-628-3p, miR-486-5p, miR-92b-5p, miR-16-3p, miR-23a-3p, and miR-23a-5p) and 4 candidate RGs (miR-21-5p, miR-221-3p, miR-16-5p, and miR-26a-5p), were performed to validate their increased expression in MRONJ patients. PCR efficiency was calculated for each gene using a linear regression model acquired from serially diluted standard samples. In analyses of expression stability, no gene showed highly stable expression; hence, genes with an intermediate level of expression stability ($0.5 < M < 1$) were considered. The two most stably expressed miRNAs (miR-21-5p and miR-221-3p) were used for normalization (Fig. 3A).

After calculating CNRQs using IRCs for each run, five targets (miR-483-5p, miR-92-5p, miR-486-5p, miR-26-5p, and miR-628-3p) showed significant differences in expression between the patient and control groups (Wilcoxon, $q < 0.05$; Table 4). As shown in Fig. 3B, miR-483-5p, miR-92-5p, and miR-486-5p were highly expressed in the MRONJ group compared to controls, whereas miR-26-5p and miR-628-3p were downregulated. Among the upregulated genes, miR-483-5p showed the largest increase (logFC = 2.340 and $q < 0.001$), followed by miR-92b-5p and miR-486-5p (logFC = 1.940 and 0.811; $q < 0.001$ and 0.008, respectively). The expression of miR-628-3p was lower in the MRONJ group (logFC = -2.140 and $q < 0.001$), in contrast to the findings from the pilot study. None of the miRNAs selected as GOIs based on previous studies, including miR-16-3p, miR-23a-3p, and miR-23a-5p, exhibited differential expression between patients and controls ($q > 0.05$). Additionally, although miR-26a-5p was included in the assay as a candidate RG based on the literature, its relative expression was significantly decreased in MRONJ patients compared to healthy individuals (logFC = -1.000 and $q < 0.001$).

Phase 3: comparison of MiRNA expression between total plasma and plasma-derived exosomes

A further experiment was conducted to assess whether the differential expression of miRNAs observed in total plasma was consistently present in plasma-derived exosomes. Exosomes were successfully isolated from all 31 plasma samples, and a qPCR assay was performed using the same targets and procedures as in the second-phase experiment. Based on the evaluation of gene stability, miR-21-5p, identified as the most stably expressed gene in total plasma, exhibited the lowest M value. However, none of the miRNAs met the stability criteria required to be used as a reliable RG, as all M values exceeded 1. Consequently, normalization was performed using the

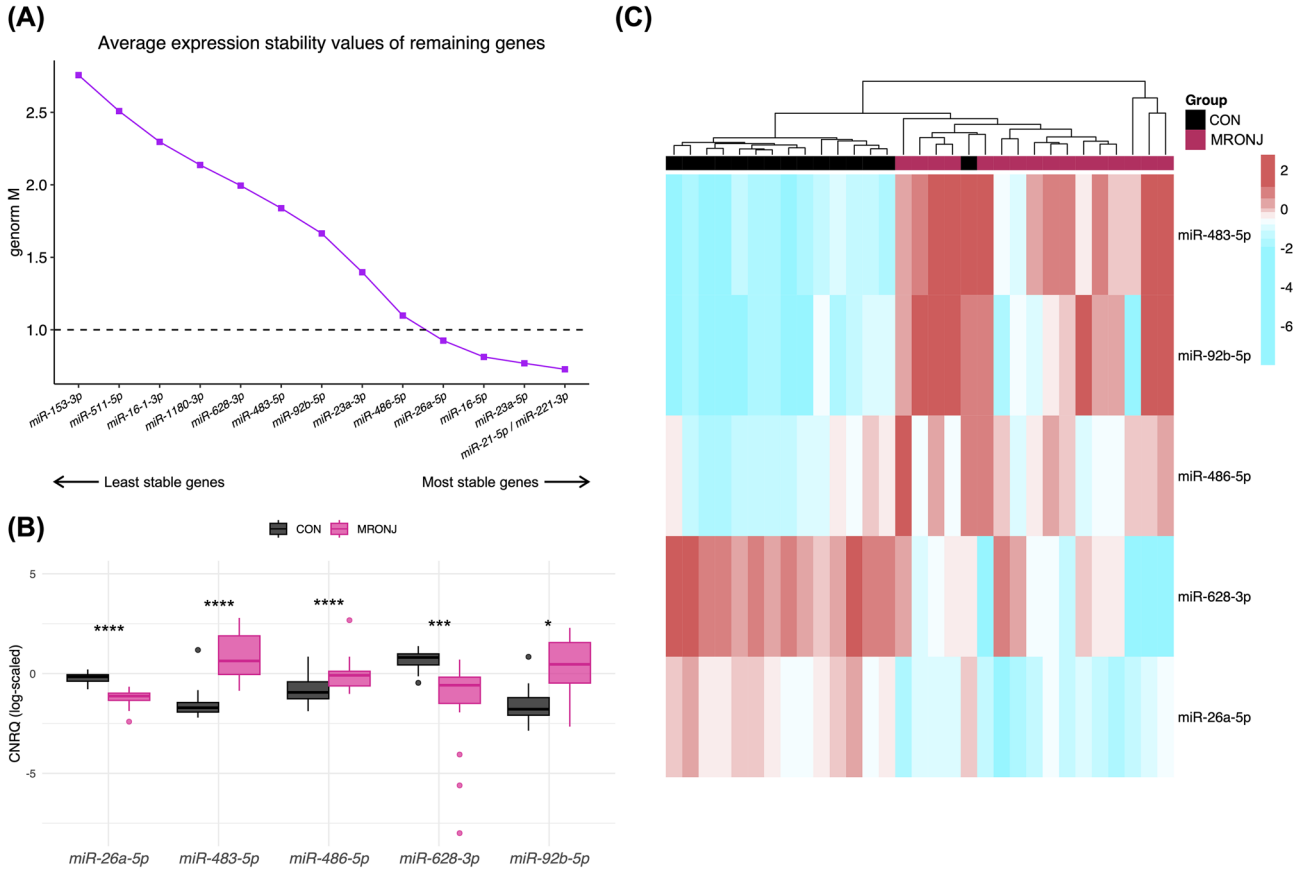

Fig. 3. Validation of selected circulating microRNAs (miRNAs) using individual quantitative real-time reverse transcriptase PCR (qPCR) assays. (**A**) The results of gene stability analysis of qPCR assay targets using the geNorm algorithm. Because no miRNA had high expression stability ($M < 0.5$), the two most stable miRNAs (miR-23a-5p and miR-221-3p) with an intermediate level of stability ($0.5 < M < 1$) were selected as reference genes. (**B**) Box plots representing the expression levels of each miRNA in patients with medication-related osteonecrosis of the jaw (MRONJ) compared to healthy controls. Among the target genes selected for the second phase, the expression levels of five genes were significantly altered in the MRONJ group compared to the control (CON) group (CNRQ, calibrated normalized relative quantity, *$Q < 0.05$, **$Q < 0.001$, ***$Q < 0.0001$). (**C**) Heatmap illustrating the differential expression of the five miRNAs between the MRONJ and control groups. Average linkage clustering based on Euclidean distances of expression values effectively distinguished the MRONJ group from the control group.

mean expression level of all target miRNAs in each sample, which enabled a consistent comparison of miRNA expression between total plasma and plasma-derived exosomes.

Among the five DE miRNAs between patients and controls in total plasma, four miRNAs displayed dysregulation in the same direction in plasma-derived exosomes. As shown in Fig. 4A, miR-483-5p, miR-92b-5p, and miR-486-5p were upregulated in both total plasma and plasma-derived exosomes of MRONJ patients compared to healthy individuals, whereas miR-628-3p was downregulated in both sample types [logFC (plasma vs. exosome) = 2.128 vs. 1.914 (miR-483-5p), = 1.726 vs. 1.862 (miR-92b-5p), = 0.596 vs. 0.361 (miR-486-5p), and = -2.354 vs. -1.924 (miR-628-3p)]. Moreover, linear mixed-effects models confirmed the consistency of these changes in miRNA expression across sample types, as the interaction between the subject group and sample type remained nonsignificant ($p > 0.05$; Fig. 4B). On the other hand, miR-26a-5p exhibited the opposite trends; the expression was higher in plasma-derived exosomes of the MRONJ group downregulated in the total plasma assay.

Discussion

For the past two decades, MRONJ has frequently been reported in clinical settings; however, our understanding of this condition remains limited, and no biomarkers for the disease have yet been identified. In the present study, in search of potential biomarkers, we identified four miRNAs (miR-483-5p, miR-92b-5p, miR-628-3p, and miR-486-5p) with significantly altered expression in both total plasma and plasma-derived exosomes of MRONJ patients compared to healthy controls. Plasma miRNA expression profiles were obtained using qPCR array plates, and findings from a literature review were considered to select 14 targets for individual qPCR assays for validation. Moreover, qPCR assays were conducted using plasma-derived exosomes to evaluate the

Gene	*P*-value*	Q-value*	logFC† (ONJ/CON)	95% CI low	95% CI high
miR-26a-5p	< 0.001	< 0.001	-1.000	-1.280	-0.716
miR-483-5p	< 0.001	< 0.001	2.340	1.610	3.070
miR-628-3p	< 0.001	< 0.001	-2.140	-3.430	-0.848
miR-92b-5p	< 0.001	< 0.001	1.940	1.070	2.810
miR-486-5p	0.003	0.008	0.811	0.226	1.400
miR-1180-3p	0.045	0.105	-0.843	-1.650	-0.035
miR-16-1-3p	0.318	0.495	-0.111	-0.901	0.679
miR-153-3p	0.401	0.561	1.230	-0.607	3.070
miR-23a-3p	0.520	0.662	0.484	-0.435	1.400
miR-16-5p	0.740	0.863	0.017	-0.347	0.381
miR-23a-5p	0.861	0.927	-0.036	-0.366	0.295
miR-511-5p	0.984	0.984	0.304	-1.080	1.690

Table 4. Validation of differentially expressed plasma MicroRNAs (miRNAs) using individual qPCR assays. FC, fold change; CON, control; CI, confidence interval. *Differentially abundant miRNAs were determined using the Wilcoxon rank-sum test, with correction for multiple testing performed using the Benjamini–Hochberg (BH) method. Statistical significance was determined as a p-value < 0.05. †The fold change value of each gene represents how many times the mean expression level in the MRONJ group is compared to the mean expression level in the control group.

consistency of miRNA dysregulation. Our results demonstrate the potential of circulating miRNA as a biomarker and highlight the need for further research in this field.

To the best of our knowledge, this study is the largest human study to date addressing circulating miRNA expression in MRONJ patients. The first human study observed upregulation of 12 genes in multiple myeloma patients diagnosed with MRONJ compared to healthy subjects[18]. Building on these findings, another study explored the feasibility of using a circulating miRNA panel as a diagnostic biomarker and proposed a predictive regression model based on three genes[19]. However, both of these previous studies had limited sensitivity for identifying candidate target genes, as they focused only on verifying previously reported targets. By contrast, we independently screened for candidate genes from 754 human miRNAs available on array plates and supplemented these with additional targets from the literature, thereby increasing the sensitivity of our screening approach. Potentially due to the different candidates, our findings are not entirely consistent with previous studies.

The four dysregulated miRNAs identified in this study were found to have regulatory effects on diverse pathways related to the hypothesized pathophysiology of MRONJ. Abundantly expressed in myocytes, miR-486-5p plays a role in cell proliferation, tissue repair, and angiogenesis[40]. By regulating downstream targets such as PTEN and FoxO1, miR-486-5p promotes cell proliferation and tissue repair; it induces angiogenesis via the downregulation of Mmp-19[41–43]. In addition, it exacerbates the inflammatory environment through NRF1 suppression and macrophage polarization, which makes it a critical factor in the pathophysiology of inflammation-related tissue damage in conditions such as rheumatoid arthritis and lipopolysaccharide (LPS)-induced inflammation[32,33]. Similarly, miR-483-5p regulates angiogenesis, cell proliferation, differentiation, and inflammation[44–46]. Its upregulation plays a pivotal role in inhibiting osteogenesis and promoting osteoclastic differentiation, thereby contributing to an imbalance in bone remodeling that favors bone resorption[26,28,31]. Increased circulating levels of miR-483-5p have been observed in patients with rheumatoid arthritis, suggesting its role in bone-related pathologies[47].

Moreover, miR-92b-5p, which is upregulated in MRONJ patients, appears to be involved in the propagation of inflammatory reactions across multiple organs. In patients with spinal cord injury, suppression of miR-92b-5p expression leads to an increase in interleukin-18-binding protein (IL-18BP) and a consequent reduction in interleukin-18 (IL-18), a pro-inflammatory cytokine that stimulates the release of other inflammatory mediators such as inducible nitric oxide synthase (iNOS), tumor necrosis factor (TNF-α), and interleukin-1β (IL-1β)[48]. A study that investigated tissue from osteoarthritis patients indicated that enhanced activity of miR-92b-5p against TIMP4 contributed to disease progression[49]. It is also reportedly involved in osteogenesis by targeting ICAM-1, indicating its association with osteoporotic conditions[30]. The function of miR-628-3p is associated with bone remodeling. In a study that compared patients with atrophic non-union to healthy controls, miR-628-3p was observed to regulate RUNX2, which plays a critical role in osteogenesis[29,50].

Altered miRNAs were also related to osteonecrosis with other causes, such as alcohol- and steroid-induced osteonecrosis of the femoral head[51,52]. Specifically, decreased expression of miR-628-3p and upregulation of miR-483-5p were observed. Taken together, in the context of MRONJ biology, the four miRNAs converge on pathways involved in osteoclast/osteoblast regulation, inflammatory signaling, and angiogenesis. These results suggest potential therapeutic avenues: antagomirs or synthetic mimics and exploring targeted delivery to modulate the oromaxillary microenvironment. From a clinical standpoint, circulating miRNAs are best positioned as complementary tools for risk stratification, prognostic assessment, and treatment monitoring rather than standalone diagnostics. These translational hypotheses will require functional validation and longitudinal evaluation to establish feasibility and clinical value.

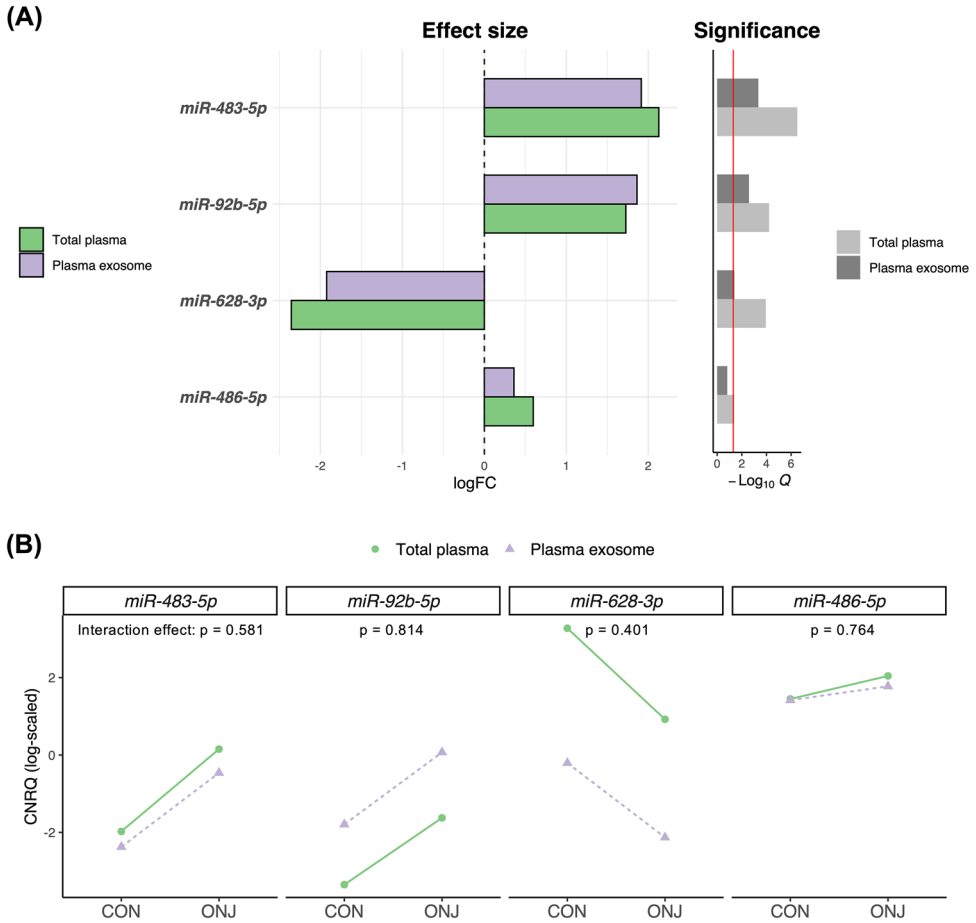

Fig. 4. Changes in microRNA (miRNA) expression in total plasma and plasma-derived exosomes of patients with medication-related osteonecrosis of the jaw (MRONJ) compared to healthy controls. (**A**) Bar plots depicting the effect size, log-scaled fold change (logFC), and statistical significance of miRNA changes in MRONJ patients across two sample types (total plasma vs. plasma exosome). Among the five miRNAs that showed significant ($q < 0.05$) dysregulation in total plasma samples from the MRONJ group, miR-483-5p, miR-92b-5p, miR-628-3p, and miR-486-5p exhibited consistent directional changes in plasma-derived exosomes. logFC values were calculated by subtracting the mean log-scaled calibrated normalized relative quantity (CNRQ) value of the control group from that of the MRONJ group, and the values from each sample type were compared for each miRNA. (**B**) Predicted log-scaled CNRQ values for subject groups (Control [CON] vs. MRONJ) and sample types (total plasma vs. plasma exosome) for the four miRNAs, estimated from linear mixed-effects models. The fitted lines represent the interaction between subject group and sample type, with each panel displaying a different miRNA target. The interaction term for each miRNA was not statistically significant (NS), indicating consistent dysregulation across sample types.

Unprecedented progress in the field of genomics has enabled researchers to dissect the human genome with greater precision, particularly in relation to non-coding RNAs such as miRNA[53]. However, the use of different methods has complicated the interpretation of data[54]. In qPCR studies, numerous methods and bioinformatics tools are available for relative quantification of gene expression[34]. In this study, we adopted the qBase + algorithm to leverage multiple RGs for normalization. In addition, standard samples were used to calculate the efficiency of each target amplification, and IRCs were applied to minimize biological and technical errors associated with PCR. For normalization, endogenous controls were carefully selected based on expression stability, as evaluated using the geNorm algorithm. Unlike exogenous spike-ins, endogenous controls are inherently present in samples and are therefore expected to behave more similarly to the target genes[35].

However, there were some limitations to this study. This study included all consecutive eligible MRONJ cases and healthy, drug-naïve controls during a defined recruitment period. Sampling was conducted at a single time point, and no prespecified matching or covariate-adjusted models were applied. Thus, some residual confounding between groups may persist. The distribution of clinical indications in enrolled cases reflected routine referrals to the participating clinics skewed toward osteoporosis with one oncology case; Stage III disease was not represented; and all included cases were women. These study features should be considered when interpreting precision and generalizability. Future work using larger, prospectively powered, multicenter cohorts with exposure-matched disease controls (e.g., osteoporosis with and without ONJ; malignancy with and without ONJ) and prespecified adjustment will enable stratified analyses by indication, regimen, route, and stage.

Plasma miRNA levels may also reflect systemic influences such as comorbidities, ongoing inflammation, medication use, metabolic state, which can bias expression patterns and complicate attribution to MRONJ alone. To improve specificity, future studies should incorporate paired tissue–plasma profiling of affected jaw sites with correlation analyses to disentangle disease–specific signals from systemic background. Finally, although we attempted to validate candidates in saliva, no meaningful data were obtained in this cohort. Since salivary miRNA profiles do not necessarily mirror plasma findings, independent saliva-focused miRNA profiling will be required to assess feasibility.

In conclusion, we identified four DE plasma miRNAs in MRONJ patients that align with pathways involved in bone remodeling, inflammation, and angiogenesis. These findings provide mechanistic insight and candidates with adjunctive potential for risk stratification, prognostic assessment, and treatment monitoring, while complementing standard clinical and radiographic diagnosis. Prospective, longitudinal, multicenter studies, incorporating baseline pre-antiresorptive sampling, serial follow-up, event-triggered collections at ONJ onset, and paired tissue–plasma profiling, are warranted to test therapeutic strategies and validate clinical applicability.

Data availability

The datasets used and/or analysed during the current study are available from the corresponding author on reasonable request.

Received: 1 July 2025; Accepted: 19 September 2025
Published online: 24 October 2025

References

1. Yarom, N. et al. Medication-related osteonecrosis of the jaw: MASCC/ISOO/ASCO clinical practice guideline. *J. Clin. Oncol.* **37**, 2270–2290 (2019).
2. Schwech, N., Nilsson, J. & Gabre, P. Incidence and risk factors for medication-related osteonecrosis after tooth extraction in cancer patients—A systematic review. *Clin. Experimental Dent. Res.* **9**, 55–65 (2023).
3. Ruggiero, S. L. et al. American association of oral and maxillofacial surgeons' position paper on medication-related osteonecrosis of the jaws—2022 update. *J. Oral Maxillofac. Surg.* **80**, 920–943 (2022).
4. Hallmer, F., Bjarnadottir, O., Götrick, B., Malmström, P. & Andersson, G. Incidence of and risk factors for medication-related osteonecrosis of the jaw in women with breast cancer with bone metastasis: a population-based study. *Oral Surg. Oral Med. Oral Pathol. Oral Radiol.* **130**, 252–257 (2020).
5. Srivastava, A. et al. Prevalence of medication related osteonecrosis of the jaw in patients treated with sequential antiresorptive drugs: systematic review and meta-analysis. *Support. Care Cancer*. **29**, 2305–2317 (2021).
6. Marx, R. E. Pamidronate (Aredia) and zoledronate (Zometa) induced avascular necrosis of the jaws: a growing epidemic. *J. Oral Maxillofac. Surg.* **61**, 1115–1117 (2003).
7. Yan, R. et al. Establishment and assessment of rodent models of medication-related osteonecrosis of the jaw (MRONJ). *Int. J. Oral Sci.* **14**, 41 (2022).
8. Lee, K. et al. Mechanisms underlying Medication-Related osteonecrosis of the jaw. *Oral Dis.* **31**, 1073–1083 (2025).
9. Moraschini, V., de Almeida, D. C. F., Figueredo, C. M. & Calasans-Maia, M. D. Association between biomarkers and medication-related osteonecrosis of the jaws: a systematic review. *Oral Surg. Oral Med. Oral Pathol. Oral Radiol.* **127**, 504–515 (2019).
10. Hirschberger, S., Hinske, L. C. & Kreth, S. MiRNAs: dynamic regulators of immune cell functions in inflammation and cancer. *Cancer Lett.* **431**, 11–21 (2018).
11. Dexheimer, P. J. & Cochella, L. MicroRNAs: from mechanism to organism. *Front. cell. Dev. Biology*. **8**, 409 (2020).
12. Liu, J. et al. MicroRNA mediated regulation of bone remodeling: a brief review. *J. Bone Mineral. Res. Plus*. **3**, e10213 (2019).
13. Das, K. & Rao, L. V. M. The role of MicroRNAs in inflammation. *Int. J. Mol. Sci.* **23**, 15479 (2022).
14. Sun, L. L., Li, W. D., Lei, F. R. & Li, X. Q. The regulatory role of micro RNA s in angiogenesis-related diseases. *J. Cell. Mol. Med.* **22**, 4568–4587 (2018).
15. Bayraktar, R., Van Roosbroeck, K. & Calin, G. A. Cell-to-cell communication: MicroRNAs as hormones. *Mol. Oncol.* **11**, 1673–1686 (2017).
16. Roi, A. et al. Circulating MiRNA as a biomarker in oral cancer liquid biopsy. *Biomedicines* **11**, 965 (2023).
17. Mohd Yunus, S. S. et al. MicroRNA in medication related osteonecrosis of the jaw: a review. *Front. Physiol.* **14**, 1021429 (2023).
18. Musolino, C. et al. Altered MicroRNA expression profile in the peripheral lymphoid compartment of multiple myeloma patients with bisphosphonate-induced osteonecrosis of the jaw. *Ann. Hematol.* **97**, 1259–1269 (2018).
19. Yang, R., Tao, Y., Wang, C., Shuai, Y. & Jin, L. Circulating MicroRNA panel as a novel biomarker to diagnose bisphosphonate-related osteonecrosis of the jaw. *Int. J. Med. Sci.* **15**, 1694 (2018).
20. Zeng, H. C. et al. MicroRNA miR-23a cluster promotes osteocyte differentiation by regulating TGF-β signalling in osteoblasts. *Nat. Commun.* **8**, 15000 (2017).
21. Hu, C. H. et al. miR-21 deficiency inhibits osteoclast function and prevents bone loss in mice. *Sci. Rep.* **7**, 43191 (2017).
22. Von Elm, E. et al. The strengthening the reporting of observational studies in epidemiology (STROBE) statement: guidelines for reporting observational studies. *Lancet* **370**, 1453–1457 (2007).
23. Vandesompele, J. et al. Accurate normalization of real-time quantitative RT-PCR data by geometric averaging of multiple internal control genes. *Genome Biol.* **3**, research0034–research0031 (2002).
24. Hellemans, J., Mortier, G., De Paepe, A., Speleman, F. & Vandesompele, J. qBase relative quantification framework and software for management and automated analysis of real-time quantitative PCR data. *Genome Biol.* **8**, 1–14 (2007).
25. Bates, D. et al. Package 'lme4'. *convergence* **12**, 2 (2015).
26. Zhao, F. et al. Silencing of miR-483-5p alleviates postmenopausal osteoporosis by targeting SATB2 and PI3K/AKT pathway. *Aging (Albany NY)*. **13**, 6945 (2021).
27. Wang, Q. et al. miR-153-3p inhibits osteogenic differentiation of BMSCs by down-regulating the expression of RUNX2 in a high glucose environment. *Am. J. Translational Res.* **14**, 7027 (2022).
28. Bellavia, D. et al. Deregulated MiRNAs in bone health: epigenetic roles in osteoporosis. *Bone* **122**, 52–75 (2019).
29. Chen, H., Ji, X., She, F., Gao, Y. & Tang, P. miR-628-3p regulates osteoblast differentiation by targeting RUNX2: possible role in atrophic non-union. *Int. J. Mol. Med.* **39**, 279–286 (2017).
30. Li, Y. et al. MicroRNA-92b-5p modulates melatonin-mediated osteogenic differentiation of bone marrow mesenchymal stem cells by targeting ICAM-1. *J. Cell. Mol. Med.* **23**, 6140–6153 (2019).
31. Li, K. et al. MiRNA-483–5p is involved in the pathogenesis of osteoporosis by promoting osteoclast differentiation. *Mol. Cell Probes*. **49**, 101479 (2020).

32. Wan, L. et al. Role of m6A modification and novel circ_0066715/miR-486-5p/ETS1 axis in rheumatoid arthritis macrophage polarization progression. *Aging (Albany NY)*. **14**, 10009 (2022).
33. Chang, Q., Ji, M., Li, C. & Geng, R. Downregulation of miR–486–5p alleviates LPS–induced inflammatory injury, oxidative stress and apoptosis in chondrogenic cell ATDC5 by targeting NRF1. *Mol. Med. Rep.* **22**, 2123–2131 (2020).
34. Marabita, F. et al. Normalization of Circulating MicroRNA expression data obtained by quantitative real-time RT-PCR. *Brief. Bioinform.* **17**, 204–212 (2016).
35. Donati, S., Ciuffi, S. & Brandi, M. L. Human Circulating MiRNAs real-time qRT-PCR-based analysis: an overview of endogenous reference genes used for data normalization. *Int. J. Mol. Sci.* **20**, 4353 (2019).
36. Damanti, C. C. et al. MiR-26a-5p as a reference to normalize MicroRNA qRT-PCR levels in plasma exosomes of pediatric hematological malignancies. *Cells* **10**, 101 (2021).
37. Gouin, K. et al. A comprehensive method for identification of suitable reference genes in extracellular vesicles. *J. Extracell. Vesicles*. **6**, 1347019 (2017).
38. Poel, D., Buffart, T. E., Oosterling-Jansen, J., Verheul, H. M. & Voortman, J. Evaluation of several methodological challenges in Circulating MiRNA qPCR studies in patients with head and neck cancer. *Exp. Mol. Med.* **50**, e454–e454 (2018).
39. Surajkulwatana, T., Vacharaksa, A., Srithanyarat, S. S. & Wongwailkhit, K. in *Proceedings of RSU International Research Conference* Vol. 1 201–211Rangsit University Pathum Thani, (2020).
40. Douvris, A., Viñas, J. & Burns, K. D. miRNA-486-5p: signaling targets and role in non-malignant disease. *Cell. Mol. Life Sci.* **79**, 376 (2022).
41. Li, Q. et al. Small extracellular vesicles containing miR-486-5p promote angiogenesis after myocardial infarction in mice and nonhuman primates. *Sci. Transl. Med.* **13**, eabb0202 (2021).
42. Bei, Y. et al. miR-486 attenuates cardiac ischemia/reperfusion injury and mediates the beneficial effect of exercise for myocardial protection. *Mol. Ther.* **30**, 1675–1691 (2022).
43. Sun, X. H., Wang, X., Zhang, Y. & Hui, J. Exosomes of bone-marrow stromal cells inhibit cardiomyocyte apoptosis under ischemic and hypoxic conditions via miR-486-5p targeting the PTEN/PI3K/AKT signaling pathway. *Thromb. Res.* **177**, 23–32 (2019).
44. Qiao, Y. et al. MiR-483-5p controls angiogenesis in vitro and targets serum response factor. *FEBS Lett.* **585**, 3095–3100 (2011).
45. Leng, C. et al. High expression of miR-483-5p aggravates sepsis-induced acute lung injury. *J. Toxicol. Sci.* **45**, 77–86 (2020).
46. Matson, K., Macleod, A., Mehta, N., Sempek, E. & Tang, X. Impacts of microRNA-483 on human diseases. *Non-coding RNA*. **9**, 37 (2023).
47. Yu, Y. et al. Exosomal hsa-mir-335-5p and hsa-mir-483-5p are novel biomarkers for rheumatoid arthritis: a development and validation study. *Int. Immunopharmacol.* **120**, 110286 (2023).
48. Lin, X. L. et al. MiR-92b-5p inhibitor suppresses IL-18 mediated inflammatory amplification after spinal cord injury via IL-18BP up-regulation. *Eur. Rev. Med. Pharmacol. Sci.* **23**, 1891–1898 (2019).
49. Lin, Z. et al. N6-methyladenosine (m6A) methyltransferase WTAP-mediated miR-92b-5p accelerates osteoarthritis progression. *Cell. Communication Signal.* **21**, 199 (2023).
50. Wei, J. et al. Experimental study of expression profile and specific role of human MicroRNAs in regulating atrophic bone nonunion. *Medicine* **99**, e21653 (2020).
51. Hong, G. et al. Analysis of Circulating MicroRNAs aberrantly expressed in alcohol-induced osteonecrosis of femoral head. *Sci. Rep.* **9**, 18926 (2019).
52. Chen, Y. et al. miR-486-5p attenuates steroid-induced adipogenesis and osteonecrosis of the femoral head via TBX2/P21 axis. *Stem Cells*. **41**, 711–723 (2023).
53. Zhang, P., Wu, W., Chen, Q. & Chen, M. Non-coding RNAs and their integrated networks. *J. Integr. Bioinform.* **16**, 20190027 (2019).
54. Siddika, T. & Heinemann, I. U. Bringing MicroRNAs to light: methods for MicroRNA quantification and visualization in live cells. *Front. Bioeng. Biotechnol.* **8**, 619583 (2021).

Author contributions

S.O., J.K., and H.L. conceived and designed the study. H.H, J.P., and K.K. contributed to sample acquisition. S.O. prepared samples, conducted PCR experiments, analyzed the data, and performed statistical analyses. S.O., M.P., J.K., and H.L. interpreted the results. S.O. and M.P. drafted the manuscript. M.P., H.H, J.P. and K.K critically revised the manuscript. All authors gave their final approval and agreed to be accountable for all aspects of the work ensuring integrity and accuracy.

Funding

This work was supported by a grant from the Korea Health Technology R&D Project through the Korea Health Industry Development Institute (KHIDI), funded by the Ministry of Health & Welfare, Republic of Korea (RS-2022-KH129467); and a National Research Foundation of Korea (NRF) grant funded by the Korea government (MSIT) (No. RS-2024-00339519) (2023R1A2C2002783).

Declarations

Competing interests

The authors declare no competing interests.

Ethical declarations

This study was approved by the Institutional Review Boards of Seoul National University Bundang Hospital and Ewha Womans University Medical Center and conducted in accordance with the Declaration of Helsinki (IRB number: B-2001-589-301 and 2021-11-020-004). All subjects provided written informed consent before participation.

Additional information

Supplementary Information The online version contains supplementary material available at https://doi.org/10.1038/s41598-025-21269-y.

Correspondence and requests for materials should be addressed to J.-W.K. or H.-J.L.

Reprints and permissions information is available at www.nature.com/reprints.

Publisher's note Springer Nature remains neutral with regard to jurisdictional claims in published maps and institutional affiliations.

Open Access This article is licensed under a Creative Commons Attribution-NonCommercial-NoDerivatives 4.0 International License, which permits any non-commercial use, sharing, distribution and reproduction in any medium or format, as long as you give appropriate credit to the original author(s) and the source, provide a link to the Creative Commons licence, and indicate if you modified the licensed material. You do not have permission under this licence to share adapted material derived from this article or parts of it. The images or other third party material in this article are included in the article's Creative Commons licence, unless indicated otherwise in a credit line to the material. If material is not included in the article's Creative Commons licence and your intended use is not permitted by statutory regulation or exceeds the permitted use, you will need to obtain permission directly from the copyright holder. To view a copy of this licence, visit http://creativecommons.org/licenses/by-nc-nd/4.0/.

© The Author(s) 2025